Dark Dunes in Martian Craters

D. Tirsch[1*], R. Jaumann[1,4], D. Reiss[1], J. Helbert[1], F. Forget[2], E. Millour[2], F. Poulet[3], R.Greeley[4] and G. Neukum[5]

[1]Institute of Planetary Research, German Aerospace Center, Berlin, Germany
[2]Laboratoire de Météorologie Dynamique du CNRS, IPSL, Université Paris 6, Paris, France
[3]Institut d'Astrophysique Spatiale, CNRS Université Paris Sud, Orsay, France
[4]School of Earth and Space Exploration, Arizona State University, Tempe, USA
[5]Planetology and Remote Sensing, Free University Berlin, Germany

*mail to : Daniela Tirsch@dlr.de

DLR German Aerospace Center

Introduction and Background

As a result of weathering and aeolian processes a fine-grained dark material can be found on both Martian hemispheres. It is characterised by a much lower albedo (< 0.15) than the surrounding terrain and accumulates in patches and dune fields. Regional scale controls such as wind regime, sand supply and climate cause different morphologies and particle sizes of the material [1]. Analysis of near infrared spectra from the OMEGA spectrometer [2] yields a higher content of mafic unoxidised minerals such as high and low Ca-pyroxenes and olivine (Fig. 1). On impact crater floors, the material is frequently accumulated into barchan or transverse dune fields. HRSC data show that the material is blown into and out of craters, indicating that such depressions can act as traps or as sources.

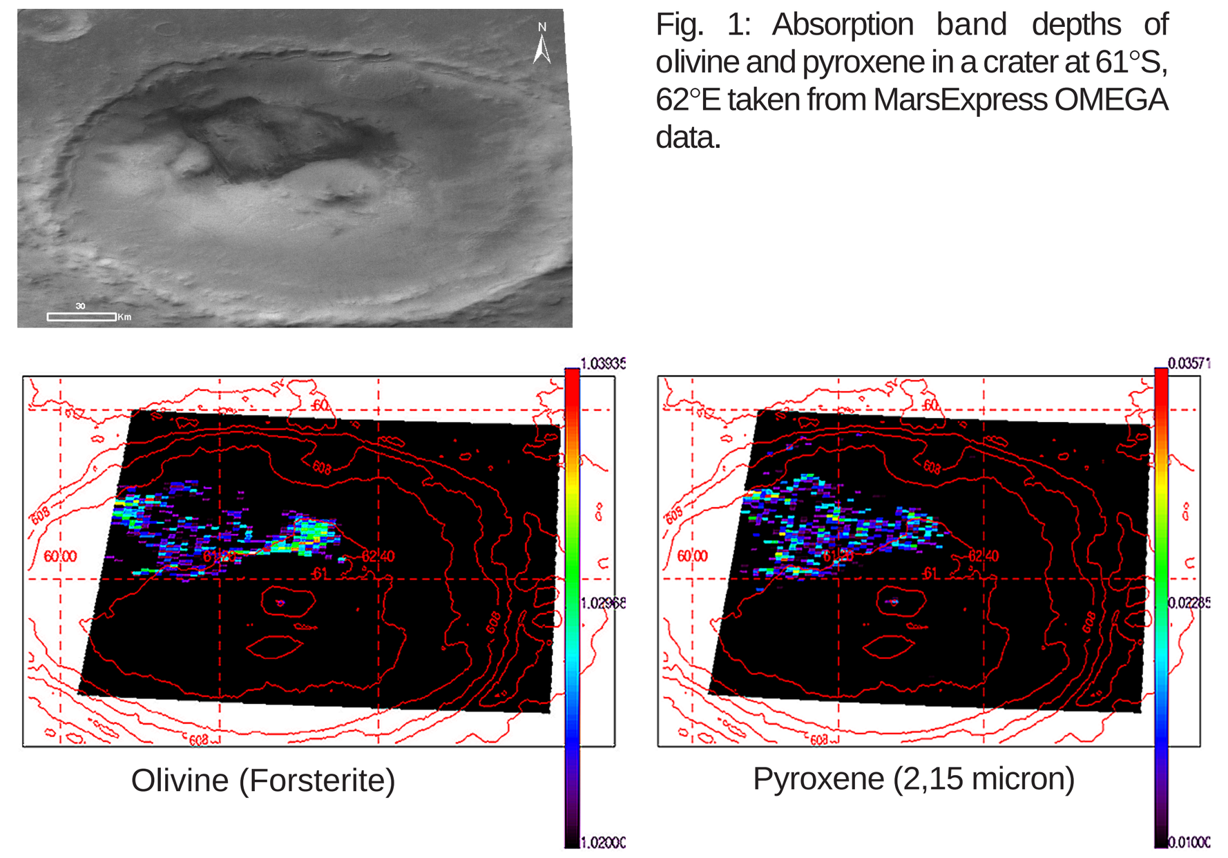

Fig. 1: Absorption band depths of olivine and pyroxene in a crater at 61°S, 62°E taken from MarsExpress OMEGA data.

Some craters have layered deposits in the crater walls which have the same albedo and the same false colour as the material inside (Fig. 2a, 2b). These dark layers could have been cut by the impact. Dark streaks running downslope (Fig. 2b) indicate that the material could be mobilised by erosion and transported onto the crater floor.

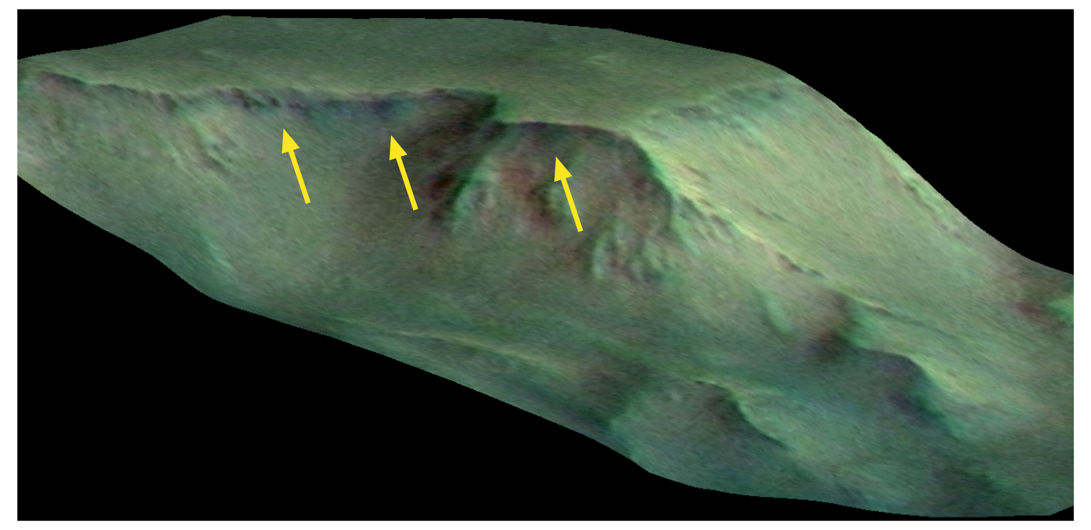

Fig. 2a: Dark layered deposits in the crater wall of a crater at 3°S, 308°E.

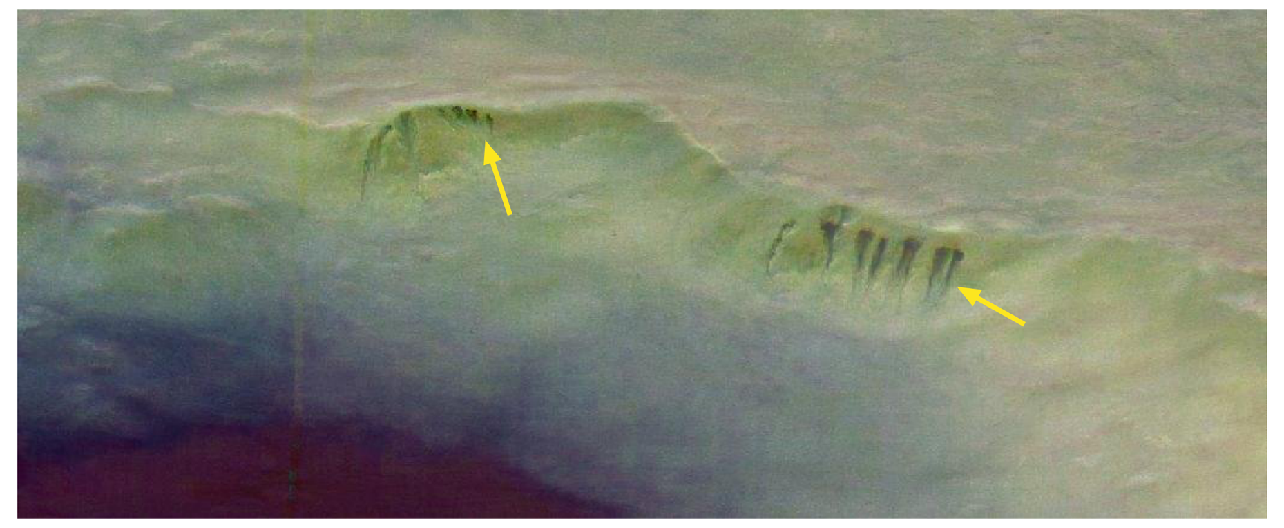

Fig. 2b: Dark layered deposits with dark streaks running downslope in the crater wall of a crater at 50°S, 247°E.

Theory

Wind direction analysis: Many dunes show dark streaks extending downwind from the dune on to its surrounding terrain indicating an unconsolidated characteristic of the material and erosion by aeolian scour. However, not every dune suggests a grain release. This poses the question if some dune surfaces are recently not influenced by the wind. We made a comparison of modeled wind fields from the Mars Climate Database (MCD) [3, 4] (Fig. 3) and the Mars Global Reference Atmospheric Model (MarsGRAM) [5] (Fig. 4) with a morphology deduced wind direction. We only took the maximum yearly amplitudes of the modeled data. The morphology deduced wind direction was easily derived from the dune shape and wind streaks.

10 m elevation				yearly mean			yearly maximum			daily mean			daily maximum		
Crater	LAT	LON (E)	Ls	amplitude [m/s]	wind direction [°]		amplitude [m/s]	wind direction [°]		amplitude [m/s]	wind direction [°]		amplitude [m/s]	wind direction [°]	
Barnard	-61,41	61,65	335,23	3,36	**129,62**	SE	7,01	**142,97**	SE	3,15	**75,81**	ENE	5,27	**57,03**	ENE
Elysium	9,63	150,13	335,77	2,1	**38**	NE	4,27	**27,33**	NNE	1,76	**20,92**	NNE	3,39	**25,37**	NNE
Tyrrhena3	-6,65	81,81	338,45	3,33	**50,57**	NE	11,05	**8,44**	N	2,58	**20,52**	NNE	4,1	**324,03**	NW
Xante1	11,95	309,68	341,12	5,93	**79,49**	E	12,17	**42,04**	NE	6,13	**48,04**	NE	11,5	**39,43**	NE
Cimmeria 1	-38,52	154,13	15,74	1,97	**160,72**	SSE	6,61	**163,8**	SSE	2,47	**168,05**	SSE	5,76	**168,16**	SSE
Ma'adim	-23,16	177,98	16,22	5,17	**250,19**	WSW	13,81	**281,14**	WNW	2,71	**128,77**	SE	4,87	**161,91**	SSE
Ophir 1	-2,98	307,81	32,5	3	**120,89**	ESE	8,51	**146,02**	SSE	2,87	**140,47**	SE	5,33	**126,63**	SE
Marte Vallis	15,58	181,58	298,66	3,2	**14,9**	NNE	9,69	**22,99**	NNE	4,62	**35,75**	NE	8,51	**29**	NNE
Argyre	-44,23	303,25	36,58	3,79	**111,85**	ESE	10,64	**108,76**	ESE	2,8	**211,36**	SSW	4,55	**131,99**	SE
Ophir 2	-7,76	303,47	37,94	3,61	**66,96**	ENE	7,24	**91,81**	E	3,12	**120,69**	ESE	6,41	**85,36**	E
Cimmeria 2	-38,13	136,42	41,98	2,2	**123,77**	SE	5,65	**192,04**	SSW	1,76	**110,09**	ESE	2,25	**148,04**	SSE
Thaumasia 1	-17,83	296,43	44,66	2,07	**315,2**	NW	4,73	**358,85**	N	2,07	**296,54**	WNW	3,63	**313,79**	NW
Thaumasia 2	-16,01	296,32	43,33	2,01	**322,69**	NW	5,48	**356,27**	N	1,79	**307,92**	NW	2,98	**345,86**	NNW
Thaumasia 2	-16,01	296,32	258,32	2,01	**322,69**	NW	5,48	**356,27**	N	2,94	**319,94**	NNW	5,12	**348,45**	N
Holden	-26,21	326,02	46,89	6	**165,17**	SSE	10,11	**146,98**	SSE	7,23	**149,48**	SSE	9,26	**148,17**	SSE
Fesenkov	21,91	273,48	151,16	3,07	**282,93**	WNW	5,6	**286,7**	WNW	3,3	**203,4**	SSW	4,37	**283,32**	WNW
Nier	43,11	106,09	155,16	1,9	**337,04**	NNW	6,45	**282,03**	WNW	1,01	**359,12**	N	1,96	**333,29**	NNW
Gill	15,8	5,4	157,25	3,77	**138,29**	SE	7,82	**219,22**	SW	3,38	**154,92**	SSE	5,85	**171,07**	S
Gill2	17,19	5,9	157,25	3,68	**145,02**	SE	7,23	**218,77**	SW	3,44	**156,09**	SSE	6,15	**172,04**	S
Kunowsky	57,08	350,34	171,75	2,25	**72,09**	ENE	6,32	**18,9**	NNE	1,64	**319,6**	NW	4,36	**321,5**	NW
Maraldi 1	-60,99	331,76	321,96	2,68	**34,87**	NE	7,58	**150,96**	SSE	2,57	**54,16**	NE	3,7	**63,96**	ENE
Perrotin	-2,85	282,07	288,96	2,04	**171,34**	S	5,02	**139,63**	SE	2,03	**318,89**	NW	2,61	**314,14**	NW
Hesperia	-31,61	108,65	246,89	4,33	**263,16**	W	11,58	**229,43**	SW	5,86	**259,46**	W	11,25	**223,37**	SW
Melas Dorsa	-21,6	290,75	49,11	3,82	**280,93**	WNW	8,93	**262,63**	W	3,48	**279,28**	W	7,29	**247,09**	WSW
Tyrrhena 1	-14,34	95,79	336,84	3,08	**326,7**	NNW	9,24	**348,38**	N	2,46	**330,94**	NNW	4,24	**324,24**	NW
Xante 2	17,97	308,99	341,12	5,12	**6,84**	N	10,62	**34,05**	NE	5,39	**3,28**	N	10,08	**34,87**	NE
Tyrrhena 2	-11,22	95,72	336,84	3,56	**20,08**	NNE	9,87	**357,68**	N	3,13	**340,86**	NNW	4,96	**354,47**	N
Marmers Valles	34,03	17,08	296,25	3,88	**215,87**	SW	7,56	**283,11**	WNW	3,41	**199,53**	SSW	5,04	**285,74**	WNW
Maja Valles	6,58	300,59	113,7	4,75	**120,36**	ESE	8,87	**164,17**	SSE	5,7	**129,25**	SE	8,7	**163,02**	SSE
Meridiani	2,15	352,16	279,7	2,83	**103,85**	ESE	7,23	**70,94**	ENE	3,9	**45,66**	NE	7,14	**70,78**	ENE
Northern	65,37	177,97	143,41	2,41	**266,77**	W	5,66	**45,89**	NE	1,2	**25,5**	NNE	3,28	**20,83**	NNE
Sinus Meridiani	1,67	8,38	246,89	3,33	**122,26**	ESE	9,27	**105,87**	ESE	4,12	**87,21**	E	8,88	**107,89**	ESE
Hellas	-51,49	66,59	253,24	2,65	**148,46**	SSE	5,55	**297,93**	WNW	2,77	**167,79**	SSE	4,95	**121,76**	ESE
Verrier	-38,37	13,16	32,5	2,97	**313,24**	NW	6,53	**276,45**	W	2,84	**299,55**	WNW	5,7	**278,81**	W
Renaudot	42,4	62,66	198,02	2,7	**217,79**	SW	5,52	**95,33**	E	2,75	**259,53**	W	3,59	**9,69**	N
Reuyl	-9,76	166,9	253,24	2,9	**178,52**	S	6,73	**168,42**	S	2,68	**314,18**	NW	6,41	**322,76**	NW
Reuyl	-9,76	166,9	257,05	2,9	**178,52**	S	6,73	**168,42**	S	2,69	**316,06**	NW	6,48	**323,42**	NW
Russell	-54,99	12,33	306,98	2,09	**337,53**	NNW	5,7	**120,05**	ESE	1,68	**98,13**	E	3,66	**126,42**	SE
Russell	-54,99	12,33	305,21	2,09	**337,53**	NNW	5,7	**120,05**	ESE	1,76	**98,67**	E	3,81	**124,81**	SE
Russell	-54,99	12,33	301,65	2,09	**337,53**	NNW	5,7	**120,05**	ESE	1,89	**99,33**	E	4,05	**122,62**	ESE

Fig. 3: Data table for the MCD data (example).

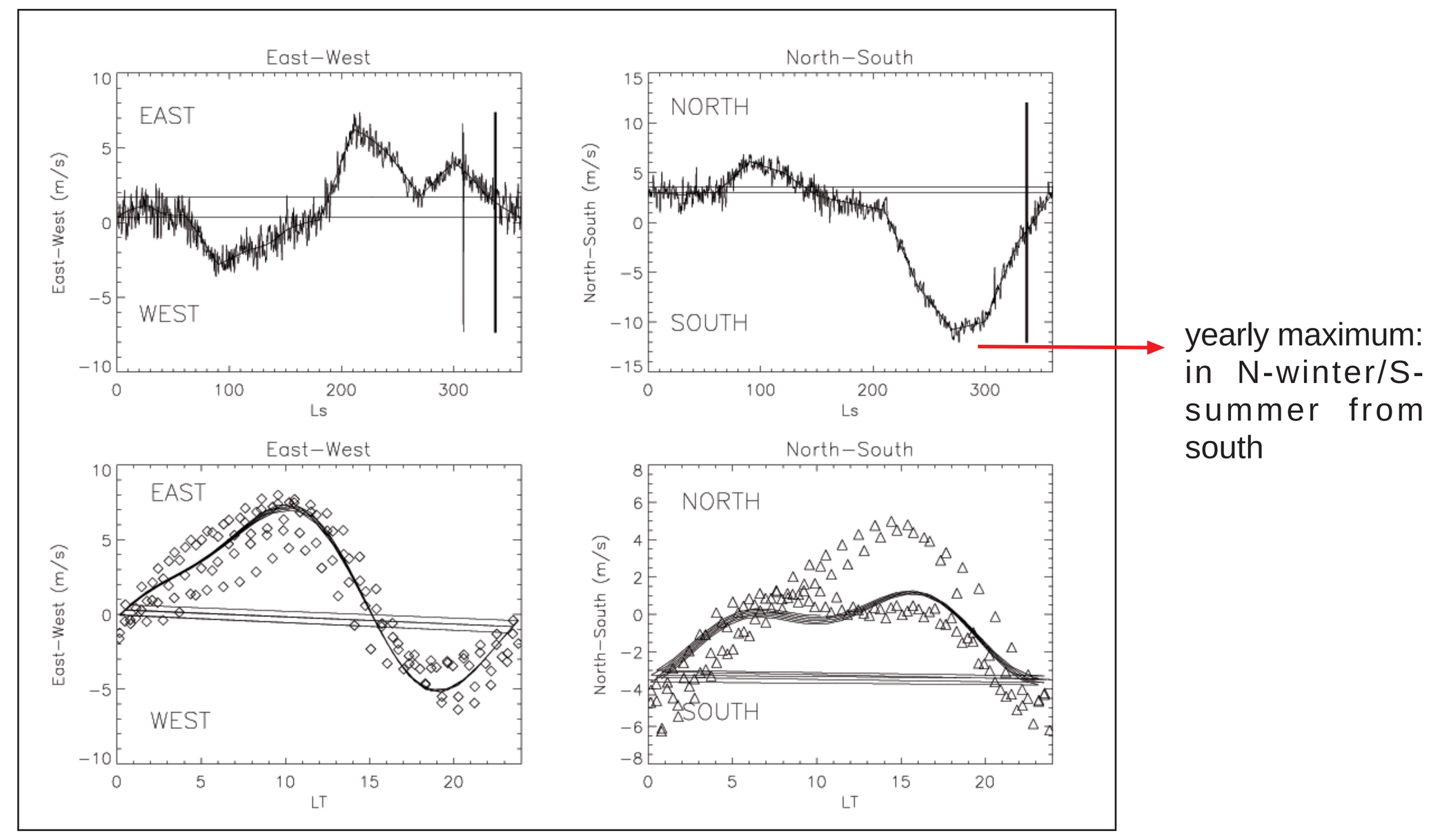

Fig. 4: Example for the MarsGRAM data for a single crater.

For more detailed information concerning the surface properties, we analysed the night-time brightness temperatures and the thermal inertia of the dune surfaces.

Brightness Temperatures (BTR): The night-time BTR from THEMIS data can provide significant information about the physical property of a dune surface in terms of a possible bonding of particles. Loose (unconsolidated) fine-grained material cools more rapidly at night than coarse-grained sediments and solid rock [6]. If the dune surfaces have warmer BTR's at night with respect to the surrounding, it can be supposed that the surface is consolidated.

Thermal Inertia (TI): The TI is a measure of a material's thermal response to the diurnal heating cycle. It is closely related to the thermal conductivity of the top few centimeters of the surface and thus directly correlated to the particle size [6, 7, 8]. We have obtained these values from TES data for all the studied craters.

Results and Discussion

Figure 5a and 6a show examples for dune fields where the dune orientation is consistent with the recent wind directions. Obviously these dark dunes are currently influenced by wind. The night-time brightness temperatures (Fig. 5b, 6b) show relative low values in comparison to the surrounding crater floor indicating that the material cools rapidly at night. The thermal inertia values of these dark dunes range between 295 - 339 $Jm^{-1}s^{-1/2}K^{-1}$ (Fig. 5c, 6c). Such low values correspond to medium to coarse sand sized material [6, 10].The results show that some dune surfaces consist of unconsolidated sandy material that is recently eroded. These dunes are supposed to be active.

Legend:

morphology deduced wind direction (red arrow)

MCD wind direction (blue arrow)

MarsGRAM wind direction (yellow arrow)

The dune orientation and the modeled wind direction are inconsistent in Figure 7a and 8a indicating that there is no obvious interaction with the current blowing winds. The higher night-time brightness temperatures (Fig. 7b, 8b) show that the material retains the heat at night. This suggests that the dune surface does not consist of loose grains. The thermal inertia values (Fig. 7c, 8c) for these dune fields range from 402 - 475 $Jm^{-1}s^{-1/2}K^{-1}$. Such high values corresponds normally to resistive outcrops and duricrusts [9, 10].

We assume that dunes with high thermal inertia values, high night-time brightness temperatures and the absence of interaction with the actual blowing wind have consolidated surfaces consisting of bounded particles.

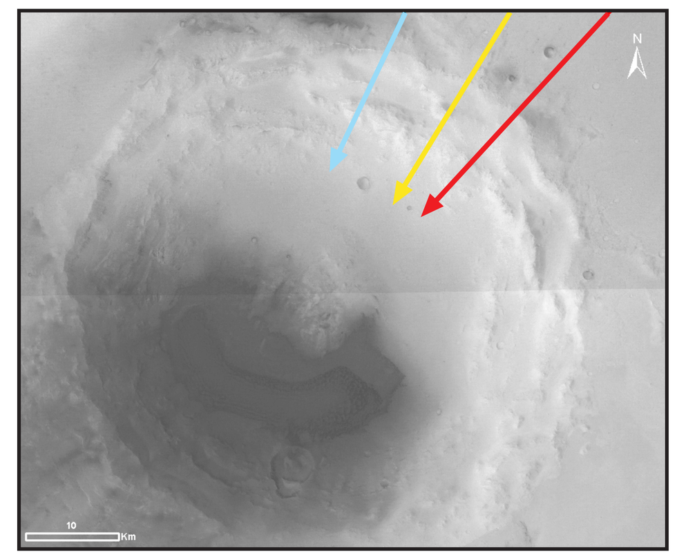

Fig. 5a: Consistent wind directions in a crater at 10° N,150°E (HRSC image, ESA/DLR/FUB).

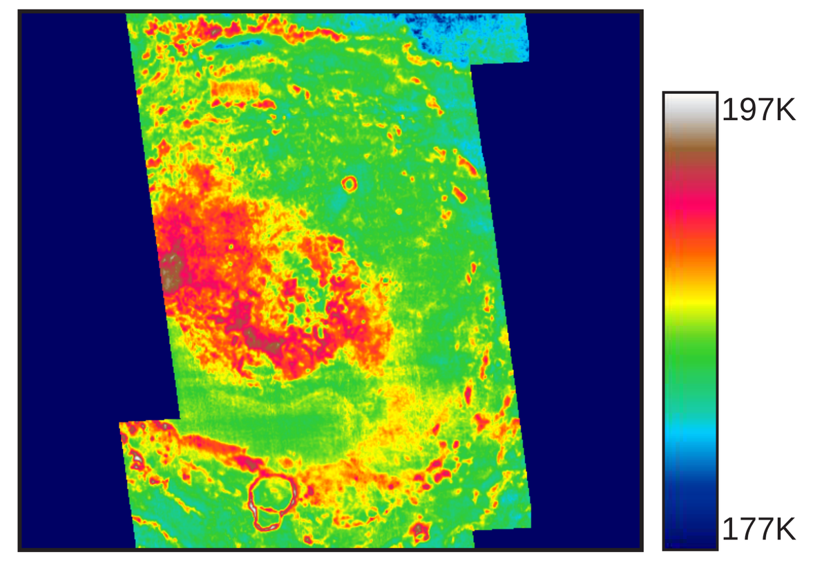

Fig. 5b: THEMIS BTR of the crater in Fig. 5a.

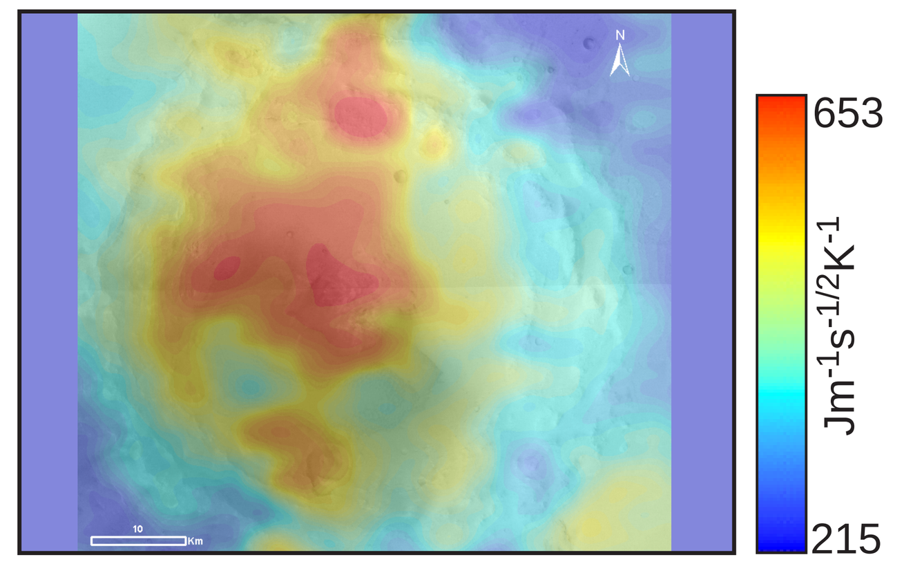

Fig. 5c: TES TI of the crater in Fig. 5a. The values for the dune field range from 318 - 339 (TES overlain onto HRSC).

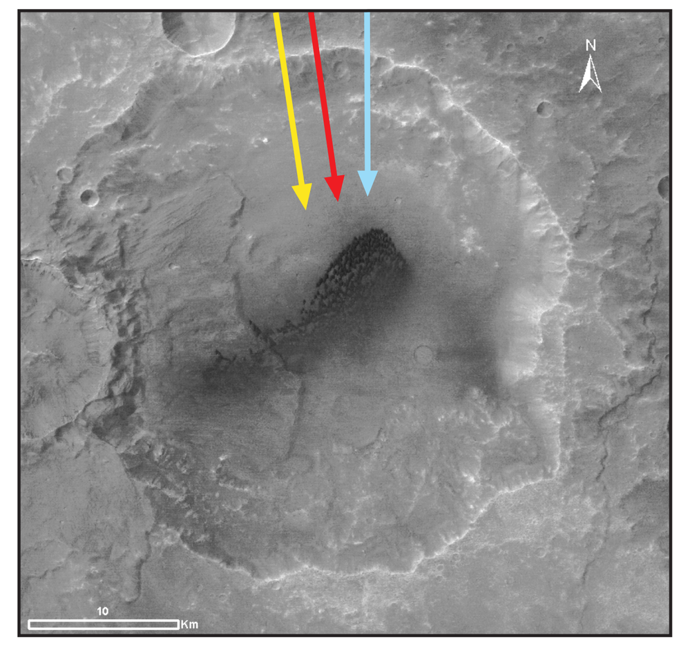

Fig. 6a: Consistent wind directions in a crater at 14°S, 96°E (HRSC image, ESA/DLR/FUB).

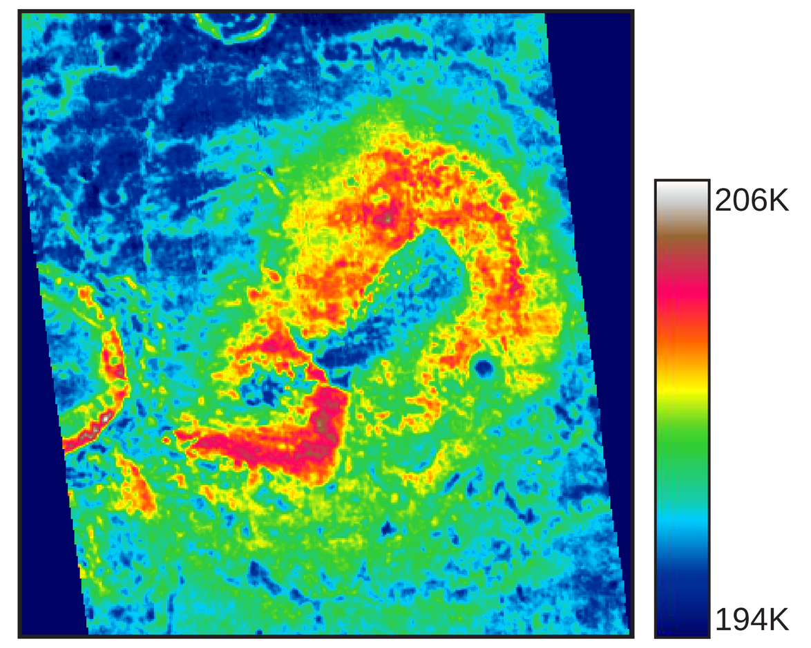

Fig. 6b: THEMIS BTR of the crater in Fig.6a.

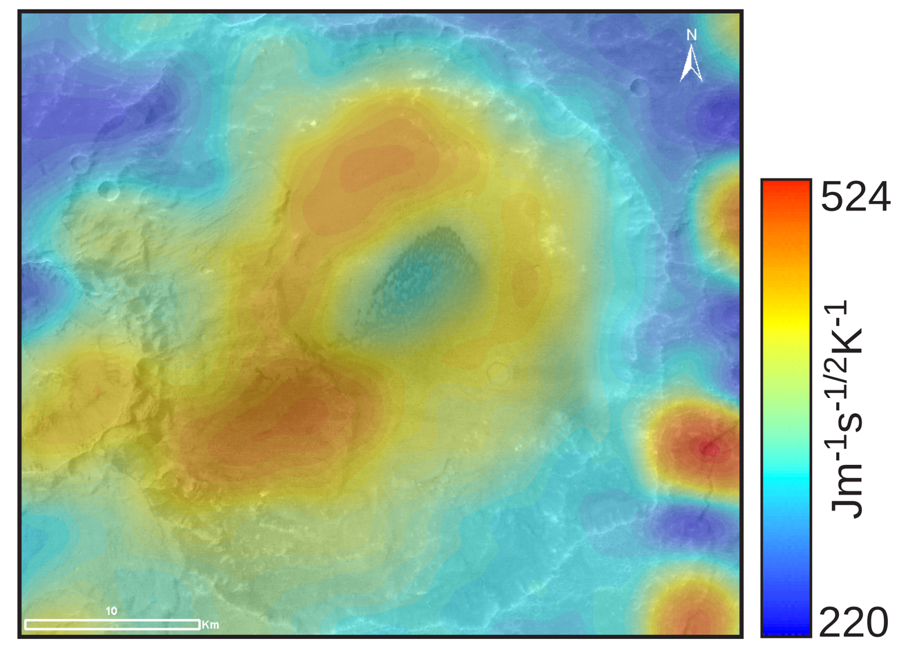

Fig. 6c: TES TI of the crater in Fig. 6a. The values for the dune field range from 295 - 305 (TES overlain onto HRSC).

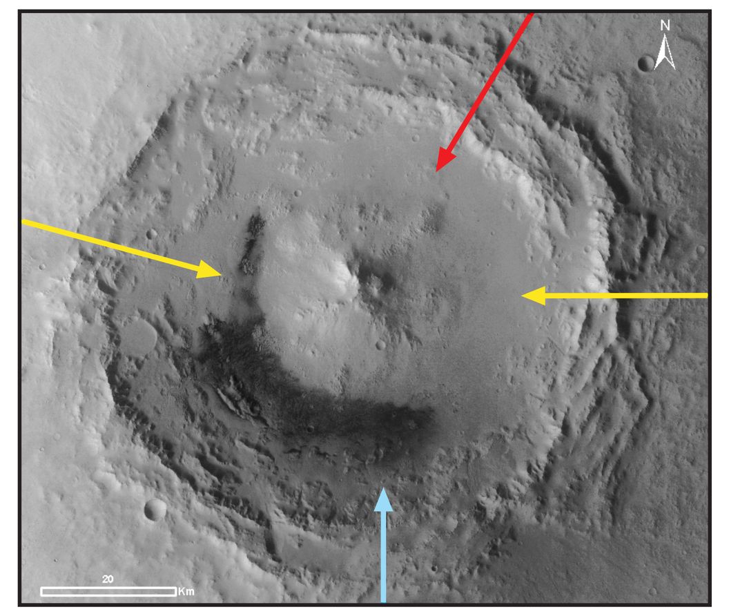

Fig. 7a: Inconsistent wind directions in a crater at 42° N, 63°E (HRSC image, ESA/DLR/FUB).

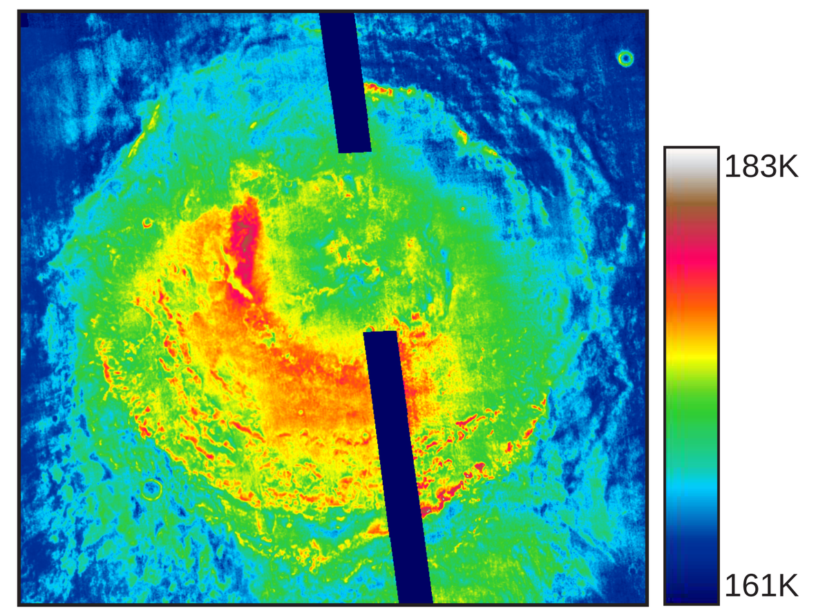

Fig. 7b: THEMIS BTR of the crater in Fig. 7a.

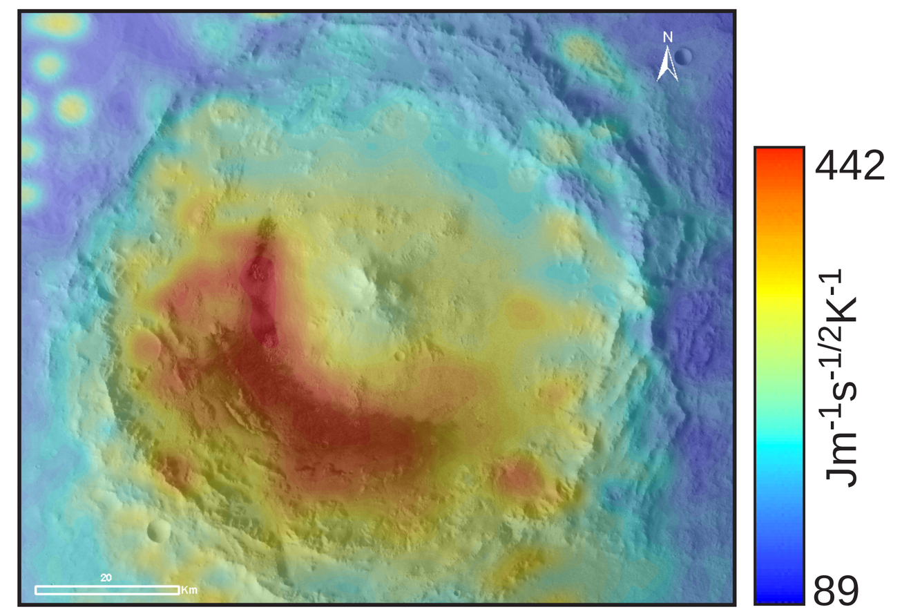

Fig. 7c: TES TI of the crater in Fig. 7a. The values for the dune field range from 402- 442 (TES overlain onto HRSC).

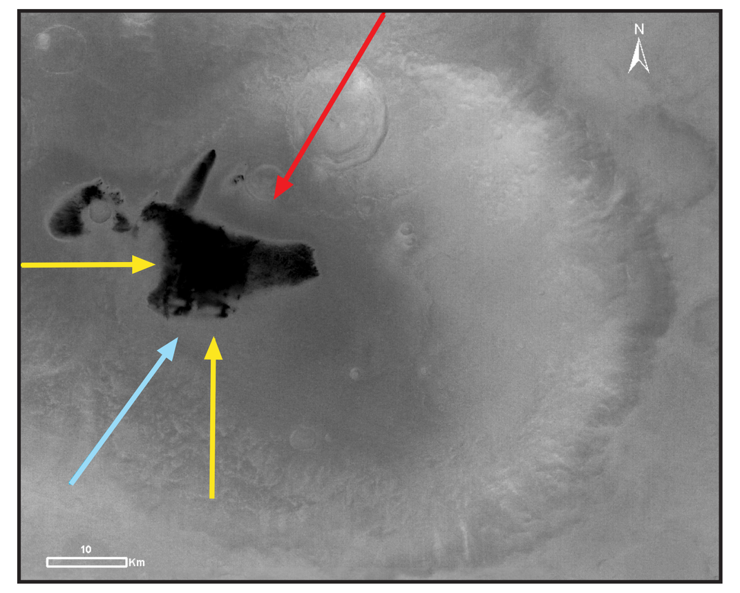

Fig. 8a: Inconsistent wind directions in a crater at 17° N, 6°E (HRSC image, ESA/DLR/FUB).

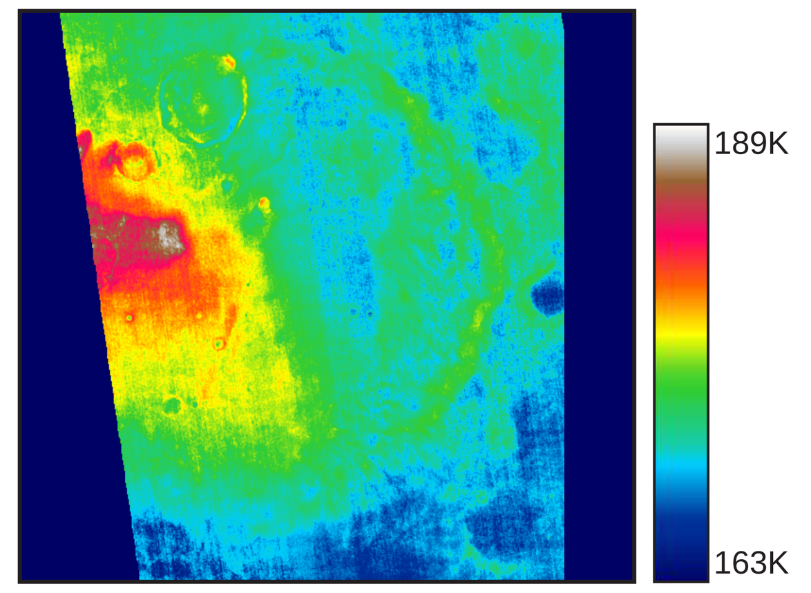

Fig. 8b: THEMIS BTR of the crater in Fig. 8a.

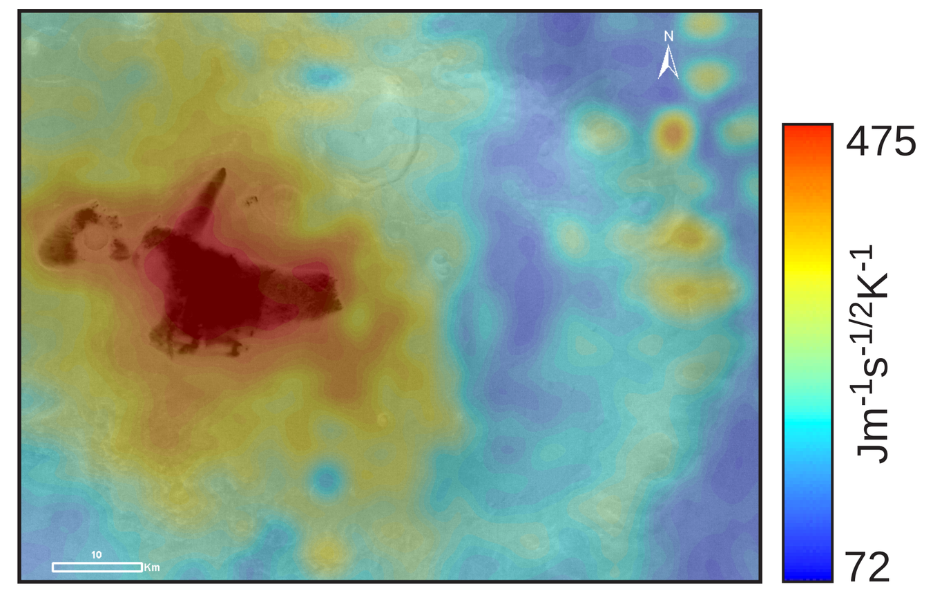

Fig. 8c: TES TI of the crater in Fig. 8a. The values for the dune field range from 411 - 475 (TES overlain onto HRSC).

The result of the analysis is shown in Figure 9. There seems to be a slightly correlation between unconsolidated dunes and the southern highlands and consolidated dunes and lower elevations, respectively. Furthermore there seems to be a certain concentration of consolidated dunes in the area of Meridiani Planum and Chryse Planitia.

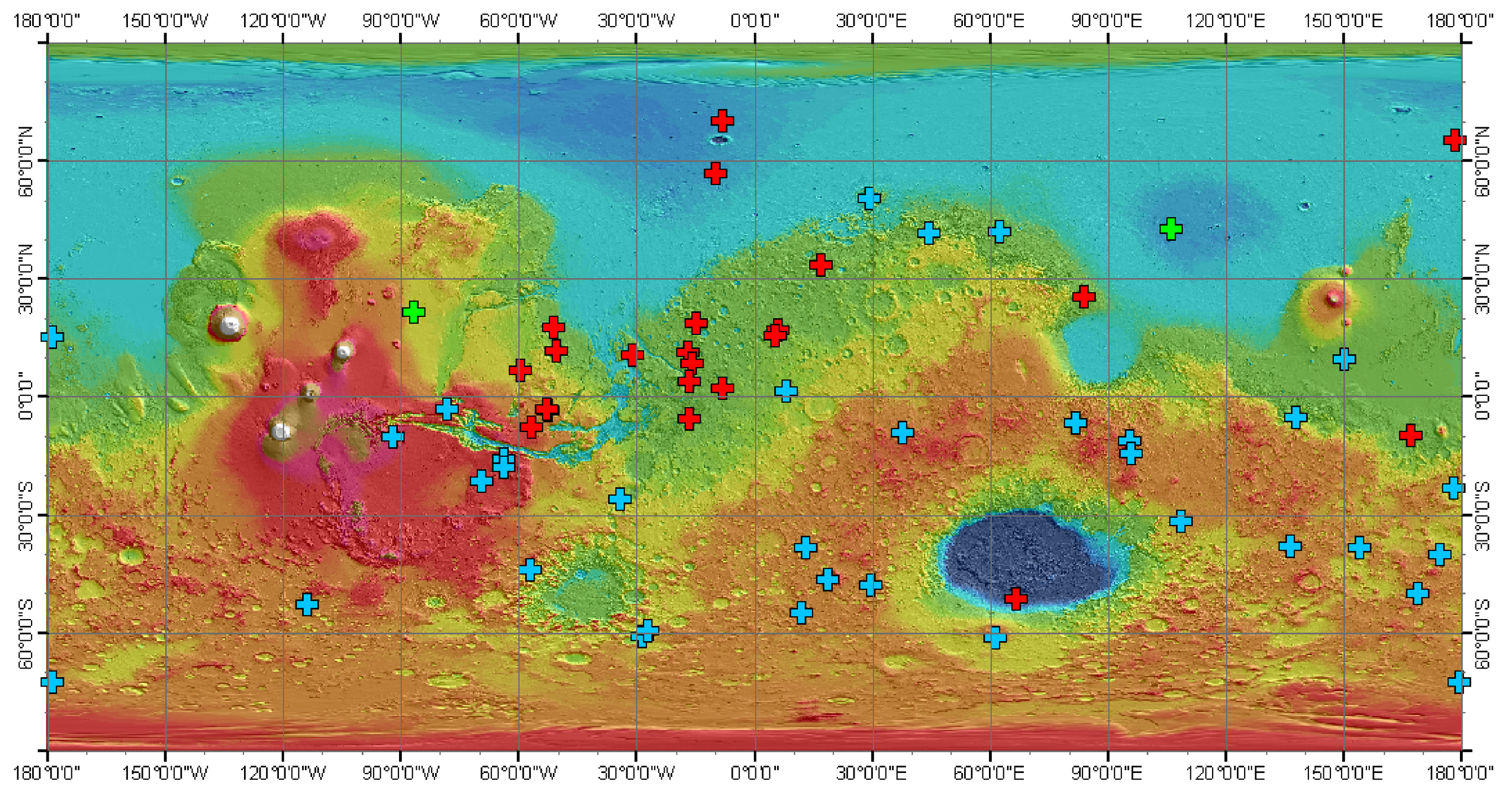

thermal inertia < 380 ⟶ unconsolidated?
thermal inertia > 400 ⟶ consolidated?
unknown

Fig. 9: Global ditribution of probably consolidated and unconsolidated dune surfaces

Conclusions

The dark materials have a mafic composition and are chemically unaltered. Thus, the material is probably the result of mechanical erosion only. Therefore it has either a relative young age or it was buried during times when liquid water occurred on the Martian surface.

The studied dune fields show significant differences in night-time brightness temperatures and thermal inertia due to variations in the physical structure and the grain size of the surface material.

The results point to unconsolidated and consolidated dark deposits. This leads to the assumption that there must have been taken place a consolidation process which is unknown yet. The physical weathering of the dark layers exposed at the crater walls could be an additional source for the dark material inside of the crater.

References:

[1] Edgett, K.S. & Christensen, P.R., JGR 99, E1, 1997 – 2018, 1994.
[2] Bibring, J.P., et al., ESA SP 1240, 37-49,2004.
[3] Forget, F. et al., JGR 104, E10, 155-175, 1999.
[4] Lewis, S.R. et al., JGR 104, E10, 177-194, 1999.
[5] Justus, C.G., et al., Avd. Space Res. 29, Nr.2, 1993-202, 2002
[6] Fenton, L.K. & Mellon, M.T., JGR 11, E06014, doi: 10.1029/2004 JE002363, 2006.
[7] Pelkey, S.M., et al., JGR 106, E 10, 23909-23920, 2001.
[8] Jakosky, B.M., et al., JGR 105, E4, 9643-9652, 2000.
[9] Putzig, N.E., et a.l, Icarus 173, 325–341, 2005.
[10]Fergason, R.L., et al., LPSC XXXIV, #1785, 2003.